

## Effects of complex magnetic ripple on fast ions in JFT-2M ferritic insert experiments

K. Shinohara 1), H. Kawashima 1), K. Tsuzuki 1), K. Urata 1), M. Sato 1), H. Ogawa 1), K. Kamiya 1), H. Sasao 1), H. Kimura 1), S. Kasai 1), Y. Kusama 1), Y. Miura 1), K. Tobita 1), D. S. Darrow 2), the JFT-2M Group 1)

1) Japan Atomic Energy Research Institute (JAERI), Tokai-mura, Japan

2) Princeton Plasma Physics Laboratory (PPPL), Princeton, USA

e-mail contact of main author: shinohak@fusion.naka.jaeri.go.jp

**Abstract.** In JFT-2M, the ferritic steel plates (FPs) were installed inside the vacuum vessel all over the vacuum vessel, which is named Ferritic Inside Wall (FIW), as the third step of the Advanced Material Tokamak Experiment (AMTEX) program. A toroidal field ripple was reduced, however the magnetic field structure has become the complex ripple structure with a non-periodic feature in the toroidal direction because of the existence of other components and ports that limit the periodic installation of FPs. Under the complex magnetic ripple, we investigated its effect on the heat flux to the first wall due to the fast ion loss. The small heat flux was observed as the result of the reduced magnetic ripple by FIW. Additional FPs were also installed outside the vacuum vessel to produce the localized larger ripple. The small ripple trapped loss was observed when the shallow ripple well exist in the poloidal cross section, and the large ripple trapped loss was observed when the ripple well hollow out the plasma region deeply. The experimental results were almost consistent with the newly developed Fully three Dimensional magnetic field Orbit-Following Monte-Carlo (F3D OFMC) code including the three dimensional complex structure of the toroidal field ripple and the non-axisymmetric first wall geometry. By using F3D OFMC, we investigated the effect on the ripple trapped loss of the localized larger ripple produced by FPs in detail. The ripple well structure, e.g. the thickness of the ripple well, is important for ripple trapped loss in complex magnetic ripple rather than the value defined at one position in a poloidal cross section.

### 1. Ripple reduction by Ferritic Inside Wall

A potentially significant heat load to the first wall can occur in ITER-size machines due to toroidal field ripple arising from the discreteness of the TF coils (TFCs). The ripple reduction by using ferritic steel plates (FPs) under TFCs was demonstrated in JFT-2M [1]. In ITER, the ripple reduction method by using FPs is planned to be applied. However, it would be difficult to install FPs with perfect toroidal symmetry because of interference with other components and ports, such as neutral beam injection ports. In this situation, “N”-fold toroidal symmetry is broken, a toroidally localized larger ripple cannot be reduced and the structure of the TF ripple becomes complex. Here “N” is the number of TFCs.

As the third stage of AMTEX program [2,3], we have installed ferritic steel F82H all over the vacuum vessel inside the vacuum vessel in F.Y. 2001 and have started the experiments from April in F.Y. 2002 [4]. This configuration is a demonstration of the ferritic steel blanket wall. Most of FPs under TF coils outside vacuum vessel was removed. We reduced the magnetic ripple by optimizing the thickness of FPs. Though the FPs are installed inside vacuum vessel,

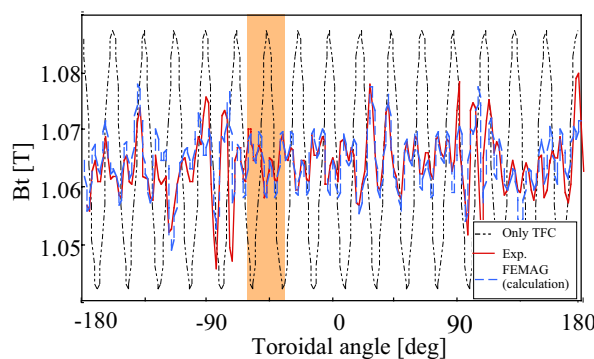


FIG.1. Shows the strength of the toroidal magnetic field at  $R=1.6$  m,  $Z=0.0$  m in the case of  $B_{t0}=1.3$  T. The horizontal axis shows the toroidal angle. The sign of the toroidal angle is positive in the direction of the counter clock-wise. The dotted line shows the toroidal magnetic field produced only by TFCs. The dashed line shows the value calculated by FEMAG code. The solid line shows the measured value by using hall elements. Shaded area corresponds to the viewing area of the IRTV camera (around TFC-3).

the FPs do not touch plasma directly with carbon tile limiters and divertor. We refer this condition as Ferritic Inside Wall (FIW).

Figure 1 shows the strength of the toroidal magnetic field for only TFC, FIW(calculation), and FIW(experiment) at the position of ( $R=1.6\text{m}$ ,  $Z=0\text{m}$ ), which is referred as “mid” below, in the case of  $B_{t0}=1.3\text{ T}$ . In JFT-2M, the number of toroidal field coils is  $N=16$  and the period of the TF ripple in the case of only TFC was 22.5 degree. The ripple amplitude defined as  $\delta=(B_{\max}-B_{\min})/(B_{\max}+B_{\min})$  for only TFC was about 2 %. The ripple structure of FIW has no periodicity in the toroidal direction and is complex because of the limitation of the installation of the FPs. The limitation comes from the compatibility with the other facilities such as the neutral beam injection system, the antenna of fast wave injection, the toroidal insulation structure, and the system of the plasma diagnostics. The ripple amplitude defined as  $(B_{\max}-B_{\min})/(B_{\max}+B_{\min})$  is not a good global indicator in this situation because  $B_{\max}$  and  $B_{\min}$  are not typical values of the complex ripple structure. Here we use the standard deviation normalized by the average, defined as  $\delta_{\text{std}} = \sqrt{\langle B^2 \rangle - \langle B \rangle^2} / \langle B \rangle$ , as an indicator of a ripple amplitude, where  $\langle \dots \rangle$  means the average over the toroidal direction. The value of  $\delta_{\text{std-mid}}$  is 0.47 % for  $B_{t0}=1.3\text{ T}$  in FIW. The ratio of  $\delta_{\text{std-mid}}$  after the installation of FIW to that of only TFCs is less than 1/3 for  $B_{t0}=1.0 - 1.9\text{ T}$ .

The measured field structure is almost consistent with that calculated by FEMAG code. It is considered the difference between the measured value and the calculated one comes from the error of the installation of FPs and the error of the measurement.

In the toroidal ripple structure produced only by TFCs, only one ripple well with a sinusoidal shape exists between two consequent TFCs. However the toroidal ripple structure formed with FPs is not simple as shown in FIG. 1. We cannot use the well-known  $\alpha$  parameter,  $\alpha=r/NRq\delta$ , simply to determine the ripple well structure, where  $r$  is the minor radius,  $N$  is the number of toroidal symmetry,  $R$  is the major radius,  $q$  is the safety factor, and  $\delta$  is the ripple amplitude defined above. Here, we define the ripple well as the existence of minimum  $B$  along a field line. At first, we determine a toroidal angle,  $\phi_s$ , at which we want to know the existence of the ripple well. Secondly we trace one of magnetic field lines from  $\phi_s$  to  $\pm \Delta\phi = 11.25(=22.5/2)$  degree. We consider the magnetic field line has a ripple well structure at the toroidal angle,  $\phi_s$ , when we encounter the stronger field than that at  $\phi_s$ . The magnetic field is determined by the following way; an axisymmetric MHD equilibrium with FPs is calculated by MEUDAS code. The magnetic field produced by TFCs and FPs is calculated by FEMAG code with magnetic field from TFCs, and poloidal field from plasma and vertical coils calculated by MEUDAS code. Figure 2 shows the ripple well structure obtained in this way and shows the case of  $B_{t0}=1.3\text{ T}$ . The ripple well exists only in a very small region of plasma reflecting the small value of toroidal ripple.

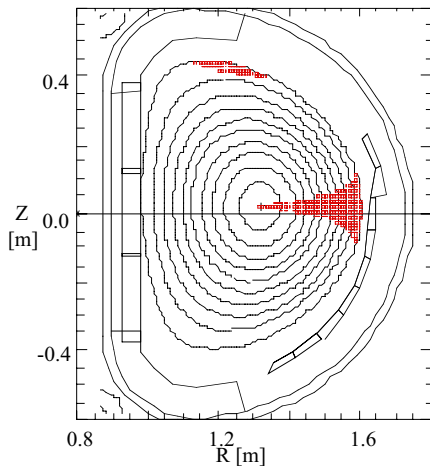


FIG.2. Ripple well structure of FIW

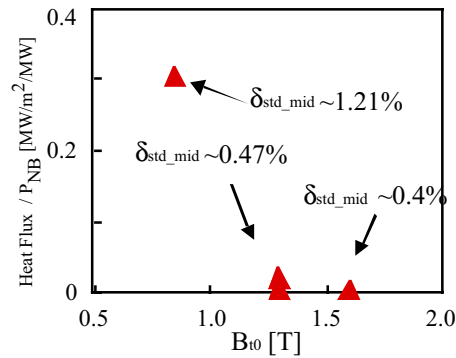


FIG.3. Heat flux normalized by NB power ( $P_{NB}$ ) at mid-plane estimated by IRTV measurement versus  $B_{t0}$

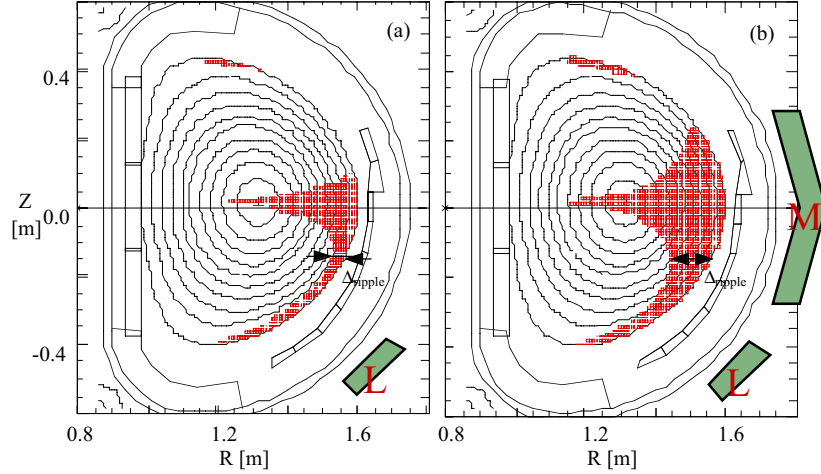


FIG.4. Ripple well structure of L EFP, (a) and M+L EFP, (b)

We injected neutral beams (NB) to this plasma configuration of FIW in the co-direction to the plasma current and the toroidal field tangentially. The power of NB ( $P_{NB}$ ) was  $\sim 0.5$  MW. The plasma was L-mode and the plasma parameters are  $\bar{n}_e \sim 2 \times 10^{19} \text{ m}^{-3}$ ,  $T_{e0} \sim 1 \text{ keV}$ ,  $T_{i0} \sim 1 \text{ keV}$ ,  $q_{95} \sim 4$ , the slowing-down time is  $\sim 30$  ms. We measured the temperature increment on the first wall by the IRTV camera. The temperature increase was observed only near mid-plane. This is consistent with the ripple well structure. Because it was expected most loss be the banana drift loss and the direct loss from the ripple well structure.

Ferritic steel F82H produces the saturated magnetic field of 1.96 T at the external field of 0.25 T. Thus the ripple amplitude is changed when the magnetic field produced by TFCs is changed. The value of  $\delta_{\text{std-mid}}$  is about 1.21% and 0.4% for  $B_{t0} = 0.85 \text{ T}$  and  $B_{t0} = 1.6 \text{ T}$ , respectively. Figure 3 shows the heat flux normalized by  $P_{NB}$  at the mid-plane estimated by the IRTV measurement for  $B_{t0} = 0.85 \text{ T}$ , 1.3 T, and 1.6 T. The value of  $\delta_{\text{std-mid}}$  is also shown in FIG. 3. The heat flux at the mid-plane is small at  $B_{t0} = 1.3 \text{ T}$  and 1.6 T, around which FIW is optimized, and is large when  $B_{t0} = 0.85 \text{ T}$  which is out of the optimum toroidal field.

## 2. Effect of Local Ripple

Localized larger ripple structure is expected to be used for the ripple-injection [5], the ripple-fueling [6] or *He* exhaust control [7] in the theoretical studies. However the experiment under the localized larger ripple was few. In the PLT tokamak, it was found that a localized larger ripple had little effect on the global confinement of tangentially injected beam ions in the experiments with the accident to one of TFCs [8]. However, the effect of fast ions on the first wall was unclear. We have produced the localized larger ripple by installing the external ferritic plate (EFP). The EFPs have been installed outside the vacuum vessel under TFC-3 ( $\phi_s = -45$  degree). The poloidal section is inside the viewing area of the IRTV camera. We have produced two types of ripple structures. In the first case, EFP is installed on a lower-shoulder part (L EFP). In the second case, EFP is installed on a Mid-plane part and a Lower-shoulder part (M+L EFP). Figure 4 shows the ripple well structure defined above around TFC-3. We can see the poloidal structure of ripple well have been modified by EFPs. Both cases produce the ripple well mainly below the mid-plane. And the ripple well structure for M+L EFP is similar to that proposed for the ripple-injection and the ripple-fueling.

The direction of the grad-B drift of ions is downward in experiments, thus the heat flux at the downward position of the plasma corresponds to the ripple trapped loss. Figure 5 shows the heat flux normalized by  $P_{NB}$  estimated by the IRTV measurement at the downward position of the plasma. In response to the modified ripple well structure, we observed the separated hot spot due to the ripple trapped loss, which was not observed in FIW. The ripple trapped loss

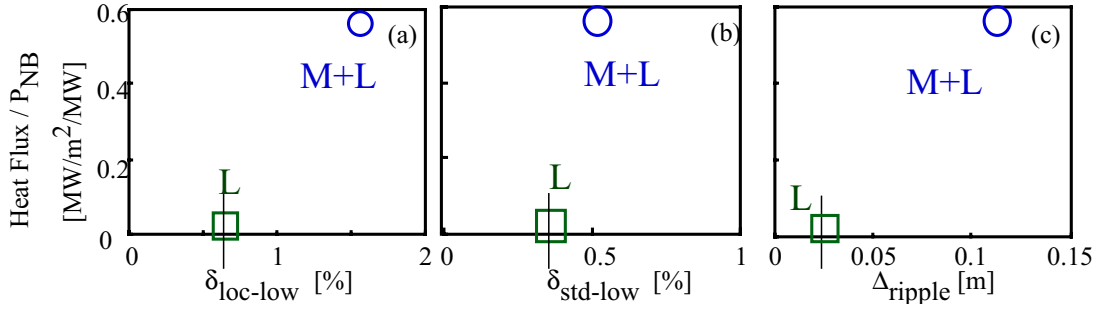


FIG.5. Heat flux normalized by  $P_{NB}$  estimated by the IRTV measurement at the downward position of the plasma for L EFP and M+L EFP.  $\delta_{loc\_low}$  and  $\delta_{std\_low}$  are the value at the lower shoulder part of plasma,  $R = 1.55$  m and  $Z = -0.2$  m.  $\Delta_{ripple}$  is the thickness of the ripple well at  $Z \sim -0.15$  m.

increase with  $\delta_{loc\_low}$  and  $\delta_{std\_low}$ . However it looks the loss suddenly start to increase at  $\delta_{loc\_low} \sim 0.5$  % and  $\delta_{std\_low} \sim 0.4$  %. In other words, the effect of localized larger ripple on the heat flux cannot be observed till  $\delta_{loc\_low} \sim 0.5$  % and  $\delta_{std\_low} \sim 0.4$  % in this configuration. Figure 5 (c) shows the heat flux of the ripple trapped loss versus the thickness of the ripple well at  $Z \sim -0.15$  m ( $\Delta_{ripple}$  shown in FIG.4). It looks the thickness of the ripple well is a more appropriate parameter for the ripple trapped loss in the complex magnetic ripple than  $\delta_{loc\_low}$  and  $\delta_{std\_low}$  in this configuration. I will discuss this issue by using simulation code later.

We also compared the toroidal rotation ( $V_t$ ) and the ion temperature ( $T_i$ ) among the FIW, L EFP, and M+L EFP configurations by using the charge exchange recombination spectroscopy. We cannot see a clear effect of the localized larger ripple on  $V_t$  and  $T_i$  for OH and L-mode plasma. This result is consistent with the result observed on PLT through Fe XX [8].

### 3. Comparison with Fully three Dimensional magnetic field (F3D) OFMC

We have improved OFMC code in order to understand the heat flux to the first wall due to the fast ion loss in the complex toroidal magnetic field. So far, OFMC assumed N-fold toroidal symmetry; the toroidally periodic boundary condition was used and the area of calculation was between two TFCs. After the installation of FPs on JFT-2M, 16-fold toroidal symmetry of magnetic field is broken and the magnetic field structure is complex. We need a new tool that can treat the complex magnetic structure in order to compare the experimental observation with the classical theory that is used in the above OFMC. We have developed OFMC without N-fold toroidal symmetry. Here, we call this code Fully three Dimensional magnetic field (F3D) OFMC.

The poloidal shape of the first wall is also not axisymmetric in JFT-2M. Banana particles hit the first wall non-axisymmetrically. In F3D OFMC, we can also allow for the non-axisymmetric first wall as the boundary to estimate heat flux. As the result of including the non-axisymmetric first wall, we observed that the limiter and the limiter-like structure cut banana ions and passing ions around the mid-plane at the low field side in the results of F3D OFMC calculations. The heat flux is large and localized at the limiter and the limiter-like structure. This new feature of F3D OFMC is useful for the estimation of the heat flux due to alpha particles to the irregular structure, such as ICRF antennas, in the fusion reactor.

We compared the heat flux of the ripple trapped loss between experiments and F3D OFMC calculations. The results are shown in FIG.6. The heat flux of experiments is almost consistent with that of F3D OFMC calculations. We also compared the poloidal structure of the heat flux of the ripple trapped loss between experiments and F3D OFMC calculations. The poloidal structure of the heat flux of experiments is also almost consistent with that of F3D OFMC calculations.

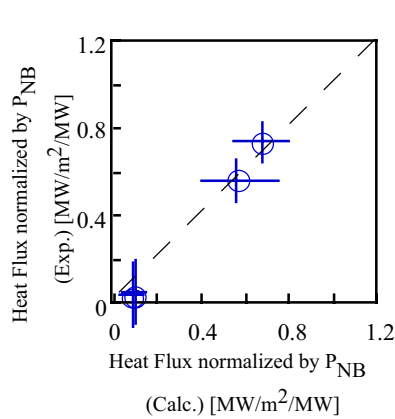


FIG. 6. The comparison of the heat flux of the ripple trapped loss between experiments and F3D OFMC calculations.

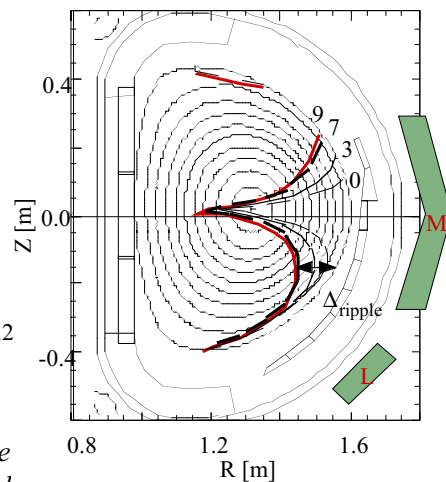


FIG. 7. Ripple well structures for the various thickness of M EFP. The M EFP is divided to nine plates. The number near ripple wells means the numerator; namely 9 means full thickness of M EFP, 3 means 1/3 thickness of full M EFP.

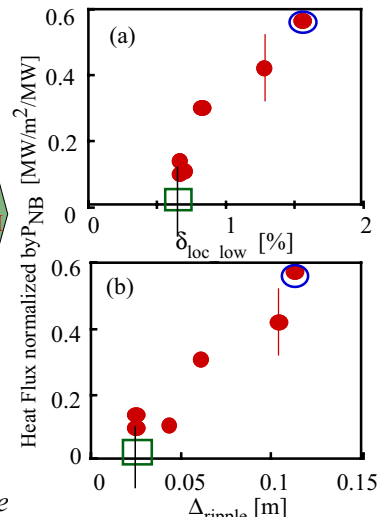


FIG. 8. The heat flux of the ripple trapped loss versus  $\delta_{loc-low}$ , (a), and the thickness of the ripple well at  $Z \sim -0.15$  m, (b). Closed circle: F3D OFMC, Open markers: Experiments

We compared the total loss of fast ions between FIW and only TFC cases at  $B_{t0}=1.3$ T by using F3D OFMC. The total loss in the case of FIW is about 1/3 as large as that in the case of only TFCs in responding to the reduction of the toroidal magnetic ripple.

In the experiments, it looks the ripple trapped loss suddenly start to increase at  $\delta_{loc-low} \sim 0.5$ . We expected the shape of the ripple well is an important feature. We have run F3D OFMC in the various thickness of M EFPs in order to change ripple well structure in a poloidal cross section. Figure 7 shows the ripple well structures for the various thickness of M EFP. Figure 8(a) shows the heat flux of the ripple trapped loss versus  $\delta_{loc-low}$ . The heat flux start to increase at  $\delta_{loc-low} \sim 0.5$  %. The experimental results are consistent with F3D OFMC calculations. Figure 8(b) shows the heat flux of the ripple trapped loss versus the thickness of the ripple well at  $Z \sim -0.15$  m. The ripple trapped loss is almost proportional to the thickness of the ripple well of the localized larger ripple. The population of fast ions is larger at a smaller minor radius. Therefore it is considered that a larger amount of fast ions can be trapped in the localized ripple when the thickness of the ripple well is thicker. From this results, the ripple well structure, e.g. the thickness of the ripple well, is important for ripple trapped loss in complex magnetic ripple rather than the value defined at one position in a poloidal cross section, which is applied in simple magnetic ripple produced by TFC. And it is also considered the FP installation near mid-plane might be enough for the reduction of the ripple induced loss of ITER through the reduction of the thickness of the ripple well.

- [1] KAWASHIMA, H., et al., Nucl. Fusion. **41** (2001) 257.
- [2] SATO, M., et al., J. Plasma Fusion Res. **75** (1999) 741.
- [3] Ninomiya, H. et al., Fusion Sci. Tech. **42** (2002) 7.
- [4] TSUZUKI, K., et al., IAEA-CN-94/EX/C1-1, this conference.
- [5] JASSBY, D. L. and GOLDSTON, R. J., Nucl. Fusion **16** (1976) 613.
- [6] TANI, K., et al., Fusion Tech. **21** (1992) 103.
- [7] HAMAMATSU, K et al., Plasma Phys. Control. Fusion **40** (1998) 255.
- [8] STODIEK, W. et al., in Plasma Physics and Controlled Nuclear Fusion Research 1980 (Proc. 8<sup>th</sup> Int. Conf. Brussels), Vol.1 IAEA, Vienna (1981), 9.